

B. UNIVERSITY RESEARCH PROJECTS

METAMORPHISM OF PELITES IN THE UPPER BLACK NOSSOB RIVER AREA OF THE DAMARA OROGEN

K.W. Kasch

Private Bag 13154, Windhoek, 9000

ABSTRACT

Four metamorphic zones are distinguished in the upper Black Nossob River area of the eastern Damara Orogen. Three of the zones are located in the better exposed Onyati Mountains Schist Belt in the western portion of the mapped area. These are, from south to north, the staurolite-kyanite zone (zone I), the staurolite-sillimanite zone (zone II), and the biotite-sillimanite zone (zone III), which are separated by the kyanite-sillimanite and the staurolite-out isograds respectively. A biotite-kyanite zone (zone IV) occurs in the south-central and eastern parts of the area, the Ekuja-Otjihangwe Nappe Complex.

Phase equilibria together with garnet-biotite geothermometry and garnet-plagioclase geobarometry indicate an increase in metamorphic temperature and a decrease in pressure from zone I in the south to zone III in the north. However, temperatures for zones I and II are the same and they only show an increase across the staurolite-out isograd from approximately 590°C in zone II to 630°C in zone III. On the other hand the pressure in zones II and III was constant at approximately 4.5kb, but distinctly higher pressures close to 6kb were recorded for zone I.

Therefore, the kyanite-sillimanite isograd reflects a decrease in pressure from zone I into zone II, whereas the staurolite-out isograd between zones II and III corresponds to an increase in temperature at approximately constant pressure. In zone IV, temperatures between 590°C and 623°C and pressures between 6.5kb and 7.7 kb were recorded.

Metamorphic reaction textures, garnet zoning profiles, and the persistence of metastable kyanite in zones II and III suggest that the Onyati Mountains Schist Belt experienced extensive decompression during prograde metamorphism. In contrast, reaction textures and garnet zoning profiles in samples from the Vaalgras Subgroup indicate that the Ekuja-Otjihangwe Nappe Complex experienced more or less isobaric heating followed by moderate decompression during and after the peak of metamorphism.

1. INTRODUCTION

The metamorphic grade in the Damara Orogen increases from the north and the south towards the Central Zone, where high-grade conditions were reached and extensive partial melting occurred (Hoffer, 1978; Hornes and Hoffer, 1979; Kasch, 1983a). Two distinctly different prograde patterns are developed, reflecting a gross asymmetry in the regional metamorphism across the orogen. Relatively high pressure conditions have prevailed in the southern Damara Orogen, whereas the pressure was distinctly lower in the central and northern portions. The peak metamorphic temperature was more or less constant in most parts of the Khomas Zone (Fig. 1), in which the assemblage kyanite + staurolite + garnet + biotite + muscovite + quartz is common. In contrast the pressure decreased from 7-10 kb along the southern edge of the Khomas Zone to approximately 4kb near its northern edge (Kasch, 1983a).

Both microtextural evidence and a quantitative reconstruction of the metamorphic history suggest that parts of the southern Damara Orogen have experienced two regional metamorphic events, which were separated by a decrease in temperature (Kasch, 1983b,c). This contrasts with the interpretation by Hoffer (1978), who has suggested that the Damara Orogen as a whole experienced a single prolonged event of regional metamorphism.

The upper Black Nossob River area is located in the eastern parts of the Damara Orogen of central SWA/Namibia between Okahandja and Steinhausen (Fig. 1).

The aim of the present investigation was to map metamorphic zones in the upper Black Nossob River area and to study the regional variation in temperature and pressure by quantitative geothermometry and geobarometry. Furthermore an attempt has been made to compare and contrast the tectonothermal evolution of the major tectonic units of this area.

2. GENERAL GEOLOGY

The upper Black Nossob River area has been subdivided into three major tectonostratigraphic units (Kasch, 1986). The lowermost unit is the Ekuja-Otjihangwe Nappe Complex, which underlies the southern, central, and eastern portions of the area (Fig. 2). The Onjona-Eleksie Nappe Complex occurs in the central, northern and north-eastern parts, while the uppermost unit, the Onyati Mountains Schist Belt, is exposed in the west and north-west. Except for the Onyati Mountains Schist Belt, outcrops in the mapped area are rather poor.

The Ekuja-Otjihangwe Nappe Complex is essentially made up of basement gneiss and a relatively thin cover of Damara Sequence metasedimentary and volcanic rocks, which has been correlated with the Vaalgras Subgroup of the Southern Margin Thrust Belt (Kasch, 1986). Major thrusting has resulted in a repetition of this basement-cover sequence, suggesting that the Ekuja-Otjihangwe Nappe Complex is part of the Southern Margin Thrust Belt.

The Onjona-Eleksie Nappe Complex and the Onyati Mountains Schist Belt are both regarded as part of the

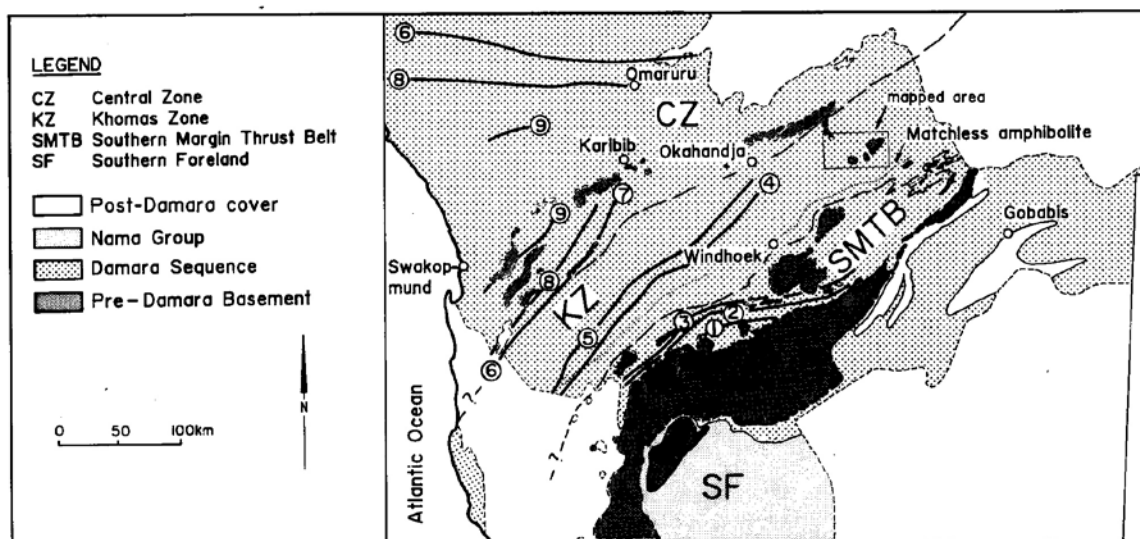


Fig. 1: Metamorphic map of the Damara Orogen (after Hoffer, 1978; Hoernes and Hoffer, 1979; Kasch, 1983a,c; Sawyer, 1981). Prograde reactions with increasing metamorphic grade are:

- (1) chlorite + plagioclase + muscovite = garnet + biotite + quartz + H₂O
- (2) garnet + chlorite + muscovite = staurolite + biotite + H₂O
- (3) staurolite + chlorite + muscovite + quartz = kyanite + biotite + H₂O
- (4) kyanite = andalusite
- (5) staurolite + muscovite + quartz = sillimanite + garnet + biotite + H₂O
- (6) andalusite = sillimanite
- (7) muscovite + quartz = K-feldspar + sillimanite + H₂O
- (8) biotite + sillimanite + quartz = cordierite + K-feldspar ± garnet + H₂O
- (9) biotite + cordierite + plagioclase + K-feldspar + quartz = melt + garnet.

Khomas Zone and are separated from the underlying Ekuja-Otjihangwe Nappe Complex by the Hochberg Thrust (Fig. 2). Intensely foliated basement gneiss and coarse-grained quartzite, marble, calc-silicate rock and minor schist make up the Onjona-Eleksie Nappe Complex. The proposed correlation of the glassy quartzite with the Nosib Group of the Central Zone (Martin, pers. comm., 1985) is uncertain, but the overlying marble and calc-silicate rock unit is correlated with the lower or middle portions of the Swakop Group. The Onyati Mountains Schist Belt consists of a very thick succession of intensely foliated schists belonging to the Kuiseb Formation.

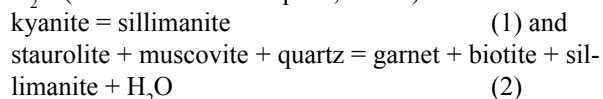
Intense deformation has produced several generations of isoclinal folds in all three zones (Kasch, 1986). However, despite some structural similarities there are also important differences. Apart from an early pre-Damara foliation in the basement of the Ekuja-Otjihangwe Nappe Complex, the earliest Damaran structures of this unit are probably younger than the D₁ and D₂ structures of the Khomas Zone. Isoclinal F₁ and F₂ folds and the penetrative s₁ and s₂ foliations of the Khomas Zone have been folded by tight and isoclinal F₃ folds. In the Onyati Mountains Schist Belt, progressive deformation during D₂ resulted in the rotation of the F₃ folds into the direction of shearing, which is parallel to a prominent west-north-westward plunging I₂ mineral lineation. A distinct northward plunging stretching lineation is associated with the Hochberg Thrust, while the F₂ and possibly the F₃ folds in the Onjona-Eleksie Nappe Complex have

been rotated into the direction of overthrusting, indicating that at least the first two phases of deformation of the Khomas Zone predate the Hochberg Thrust. The west to west-north-westward plunging and southward vergent F₃ folds together with the stretching lineations of the Hochberg Thrust indicate that thrusting of the Khomas Zone over the Ekuja-Otjihangwe Nappe Complex was from north to south.

3. METAMORPHIC ZONES AND TEXTURES

3.1 Metamorphic Zones

Mapping of metamorphic mineral assemblages in pelitic rocks of the upper Black Nossob River area has revealed significant variations in metamorphic grade. In the Onyati Mountains Schist Belt in the west, three distinct metamorphic zones which are separated by two well-defined isograds, are recognized (Fig. 3). From south to north, these are the staurolite-kyanite zone (I), the staurolite-sillimanite zone (II), and the biotite-sillimanite zone (III), which are separated by the kyanite-sillimanite and the staurolite-out isograds (Fig. 3). At these isograds the univariant reactions in the six component pelitic subsystem K₂O-FeO-MgO-Al₂O₃-SiO₂-H₂O (KFMASH of Thompson, 1976a) are



A north-south trending staurolite-out isograd in the

sillimanite + kyanite + garnet + biotite + muscovite + quartz
sillimanite + kyanite + staurolite + garnet + biotite + muscovite + quartz
staurolite + garnet + biotite + muscovite + quartz
kyanite + garnet + biotite + muscovite + quartz

Zone III

sillimanite + garnet + biotite + muscovite + quartz
sillimanite + biotite + muscovite + quartz
sillimanite + kyanite + garnet + biotite + muscovite + quartz
kyanite + garnet + biotite + muscovite + quartz

Although kyanite is present everywhere in the upper Black Nossob River area, it is metastable in zones II and III, where it was produced before the peak of metamorphism was reached. However, in these two zones the modal content of kyanite in the schists clearly decreases while that of sillimanite increases from south to north. Plagioclase and retrograde chlorite are usually present and accessory minerals are sphene and ilmenite, while calcite, rutile and tourmaline are occasionally found.

Typical assemblages in Zone IV are:

kyanite + garnet + biotite + muscovite + quartz

garnet + biotite + muscovite + quartz
garnet + hornblende + biotite + muscovite + epidote + quartz.

Outcrops of kyanite-bearing schists in zone IV are restricted to a few localities, one of which occurs along the south-eastern slopes of Hochberg hill on the farm Hochberg 158. Plagioclase and retrograde chlorite are frequently present, and accessory minerals are sphene, ilmenite, rutile and calcite.

3.2 Metamorphic Textures

3.2.1 The Timing of Metamorphism

Textural evidence suggests that most metamorphic minerals in the Onyati Mountains Schist Belt grew during D₂ as well as after D₄.

Staurolite and kyanite frequently define a prominent I₂ mineral lineation (Kasch, 1986), which is often tightly crenulated by F₃ micro folds, and many bent kyanite crystals have been observed in thin section. Many garnets show S-shaped inclusion trails, indicating that they are syntectonic (*cf.* Zwart, 1962; Vernon, 1978). The sense of rotation of these garnets is clearly related to the

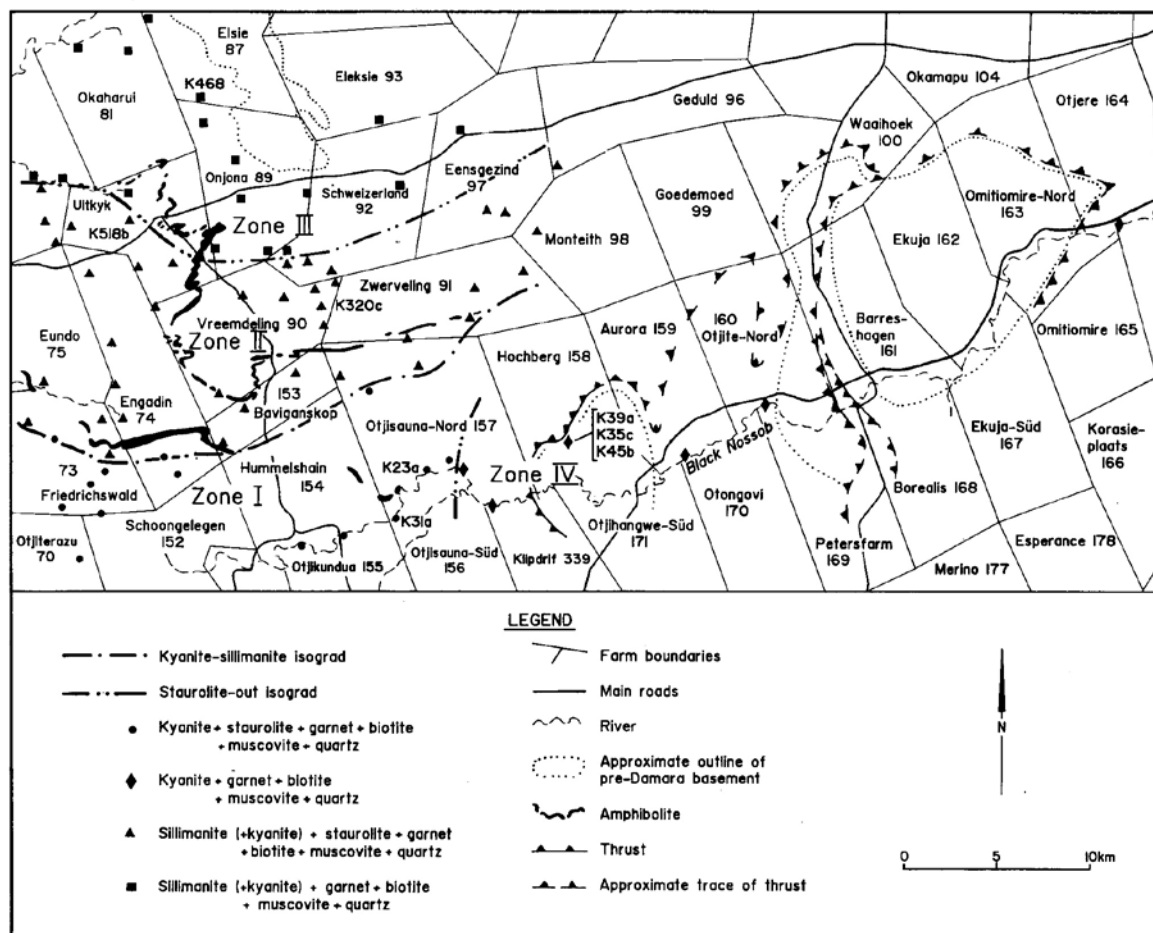


Fig. 3: Metamorphic map of the upper Black Nossob River area, showing the four metamorphic zones, the kyanite-sillimanite and staurolite-out isograds, and the sample localities.

asymmetry of F_2 microstructures in the schists, suggesting that these are syn- D_2 garnets. Several garnets have straight inclusion trails which are discontinuous with the external foliation. These are post- s_2 but pre- D_3 garnets. Biotite and muscovite flakes are oriented parallel to the s_2 foliation and deformed by F_3 micro folds. From these textures it is concluded that the Kuiseb schists in the upper Black Nossob River area experienced amphi-

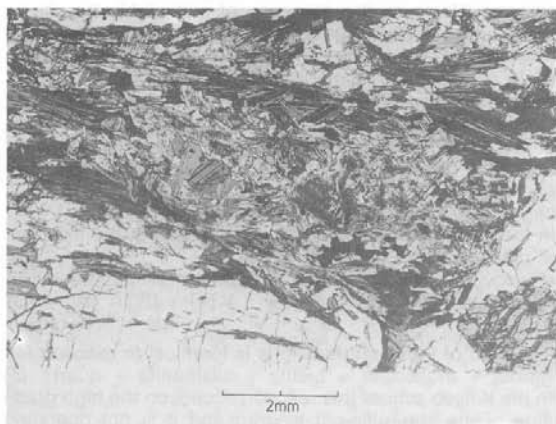


Fig. 4: Randomly oriented muscovite porphyroblasts are extensively replaced by fibrolitic sillimanite. Sample K468, Elsie 87.

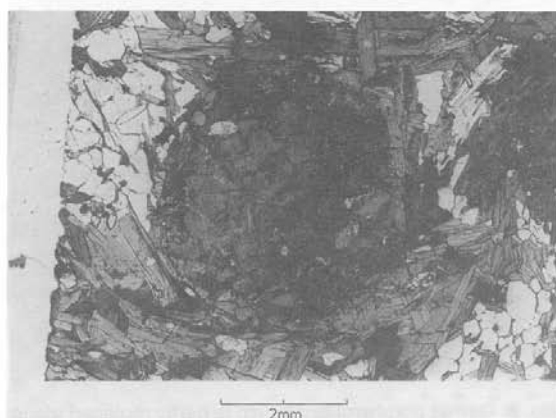


Fig. 5: Garnet porphyroblast which is almost entirely pseudomorphed by randomly oriented biotite, which in turn is extensively replaced by post-tectonic sillimanite. Sample K518b, Uityk 80.

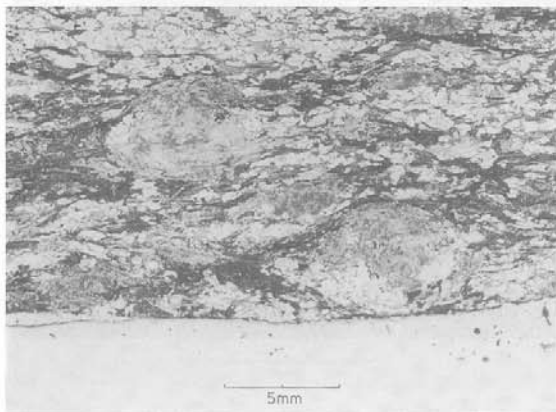


Fig. 6: Sillimanite nodules pseudomorphing garnet in a biotite-sillimanite schist. Sample K460, Onjona 89.

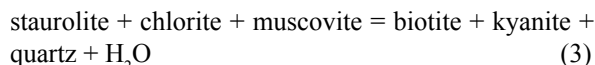
bolite facies metamorphism during and just after the second phase of deformation.

Many staurolite, kyanite, biotite, and muscovite porphyroblasts are randomly oriented and have overgrown both s_2 and s_3 foliations as well as all younger crenulations. In contrast, no post-tectonic garnets have been identified. Folded sillimanite-rich layers and quartz-sillimanite nodules, many of which are elongate and aligned parallel to l_2 , were found, suggesting that sillimanite growth was syn- D_2 . However, careful thin section studies indicate that fibrolite has replaced previously folded muscovite-rich layers. Many sillimanite nodules are pseudomorphs after elongate muscovite porphyroblasts (Fig. 4), which were previously aligned parallel to l_2 . Within these nodules sillimanite forms irregular clusters of post-tectonic fibrolite. In some instances garnets are pseudomorphed by randomly oriented biotite which in turn shows extensive replacement by fibrolite (Fig. 5). Quartz-rich pressure shadows around syntectonic garnets are aligned parallel to l_2 . Whenever these garnets are completely replaced by fibrolite, the pressure shadows are also extensively replaced (Fig. 6), again resulting in elongate nodules. Thus, in contrast to other mineral phases in the area, all the sillimanite is of post-tectonic origin, although it often gives the impression that it grew during D_2 .

Microstructures in the pelitic schists of the Vaalgras Subgroup in zone IV are similar to those in the Kuiseb schists. Again, syntectonic as well as post-tectonic kyanite, biotite, and muscovite are present, while only syntectonic garnets have been identified. It is, therefore, evident that the upper Black Nossob River area has experienced middle amphibolite facies conditions during, as well as after, the deformation.

3.2.2 Reaction Textures

Reaction textures have also been studied to provide some information on the type of mineral reactions that were responsible for the prograde assemblages observed in the upper Black Nossob River area. Both garnet and staurolite have been frequently corroded and replaced by other metamorphic minerals. Staurolite in Kuiseb Formation schists of zones I and II is often pseudomorphed or partly replaced by kyanite (Fig. 7), which in the six component pelitic subsystem KFMASH of Thompson (1976a), may be accounted for by the discontinuous reaction.



No primary chlorite is present, suggesting that chlorite was consumed by reaction (3) before all the staurolite reacted out. The metamorphic temperature in the upper Black Nossob River area is thus likely to have been higher than that required for reaction (3), and indeed Hoffer (1983) has mapped the corresponding isograd well within the Southern Margin Thrust Belt (Fig. 1).

Garnet, in contrast to staurolite, has been replaced by

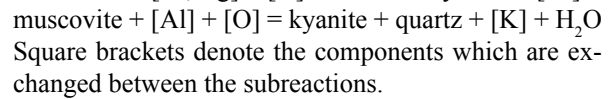
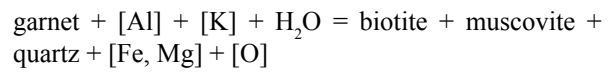
a variety of minerals, and at least two continuous reactions have been responsible for the consumption of garnet. In zone IV several garnets in the conglomerate matrix of the Hochberg Formation in the Ekuja-Otjijhangwe Nappe Complex are partly replaced by randomly oriented biotite (Fig. 8). The presence of post-tectonic kyanite which is almost in contact with garnet suggests that the continuous reaction

$$\text{garnet} + \text{muscovite} = \text{biotite} + \text{kyanite} + \text{quartz} \quad (4)$$

was responsible for the breakdown of garnet.

In the schists of the Kuiseb Formation in zones I, II and III, biotite, muscovite, and quartz have frequently grown along cracks in the core of garnets (Fig. 9). Similar textures have been described by Yardley (1977a) from the Connemara schists in Ireland. The replacement of garnet by muscovite in addition to biotite and quartz in the Kuiseb schists is a problem, because in reaction (4) both garnet and muscovite are consumed. However, Carmichael (1969) and Yardley (1977a) have shown that, on thin section scale, a particular mineral can be produced in one locality and at the same time it can be consumed somewhere else. Diffusion allows two or more of these subreactions to exchange chemical com-

ponents and together they make up the net metamorphic reaction. It is suggested, therefore, that in the Kuiseb Formation schists muscovite, biotite, and quartz have replaced garnet while elsewhere in the matrix muscovite was consumed by kyanite, biotite and quartz. Neglecting Ca, Mn, and details of Fe-Mg cation exchange, the subreactions are:



In zone III garnet is progressively replaced by sillimanite (Fig. 6) with increasing metamorphic grade and near the northern edge of the mapped area hardly any garnets are found. Very often these garnets are pseudomorphed by biotite, which is itself altered extensively to fibrolitic sillimanite (Fig. 5). Yardley (1977a) has proposed a system of subreactions within a closed ionic reaction cycle to explain similar textures. However, the presence of metastable kyanite in the Kuiseb schists suggests that in this case garnet initially reacted

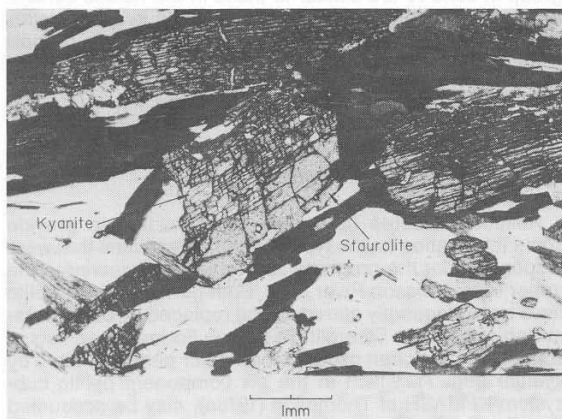


Fig. 7: Staurolite porphyroblast which is partly replaced by kyanite. Sample K23a, Otjisauna-Nord 157.

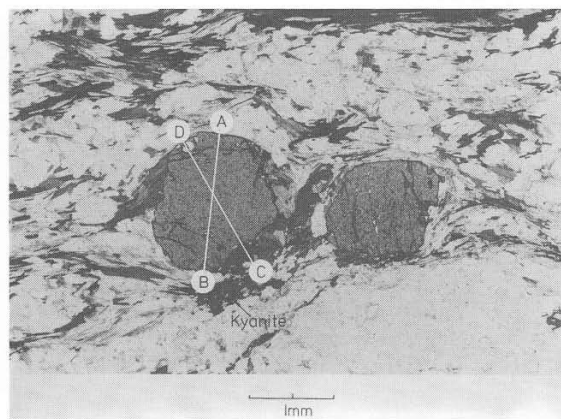


Fig. 8: Garnet porphyroblast which is partly replaced along the margins by randomly oriented biotite with post-tectonic kyanite present nearby. Sample K39a, Hochberg Formation, Hochberg 158.

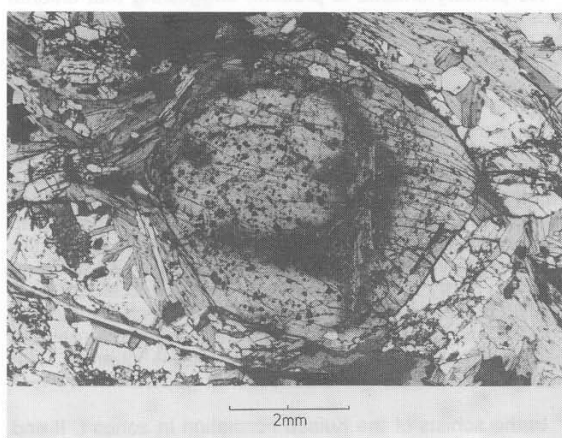


Fig. 9: (a) Biotite flakes which have grown in the centre of a garnet. Sample K518b, Uitikyk 80.

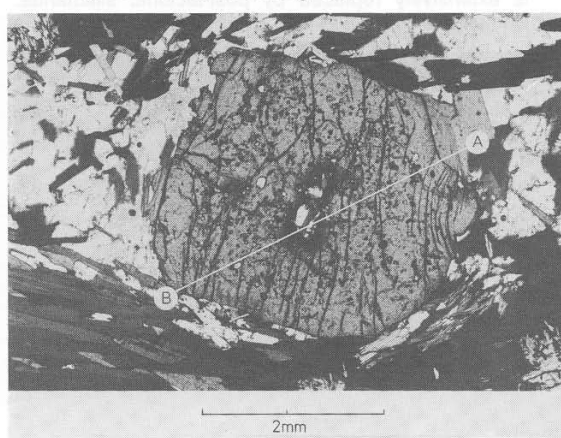
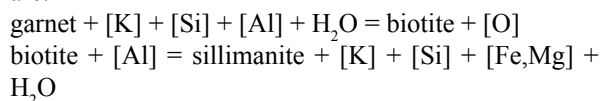
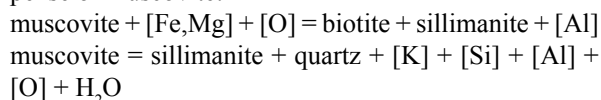


Fig. 9: (b) Biotite, plagioclase and quartz have partly replaced the core of a garnet. Sample K31a, Otjisauna-Süd 156.

with muscovite to form biotite and kyanite (reaction 4). As conditions of sillimanite stability were reached, the biotite pseudomorphing garnet was itself replaced by sillimanite accompanied by growth of new biotite in the matrix. Neglecting Ca, Mn, and details of Fe-Mg exchange reactions, the two subreactions within garnet are:



In the matrix biotite and sillimanite formed at the expense of muscovite:



The sum of these subreactions is identical to reaction (4): garnet + muscovite = biotite + sillimanite + quartz (5). In the Kuiseb schists this reaction occurs on the high grade side of the staurolite-out isograd and it is not operating simultaneously with the breakdown of staurolite as suggested by Yardley (1977a).

A whole range of garnets exists, from virtually fresh ones to those which are almost completely replaced by biotite, muscovite, and quartz. In the latter case, the randomly oriented biotite and muscovite crystals are slightly deformed, indicating that reactions (4) and (5) were late syn-tectonic (perhaps syn- D_4) to post-tectonic. This suggests that a single prolonged metamorphic event occurred, which outlasted all four events of deformation. In some instances biotite, muscovite, quartz, and plagioclase have replaced the core of garnets resulting in atoll structures (Fig. 10).

In the Onyati Mountains Schist Belt, early syntectonic kyanite was produced by the discontinuous reaction (3) during prograde metamorphism, whereas post-tectonic kyanite was formed by the continuous reaction (4) which took place during the peak of metamorphism. Several syntectonic kyanites have been partly replaced by plagioclase (Fig. 11) which indicates that the continuous reaction

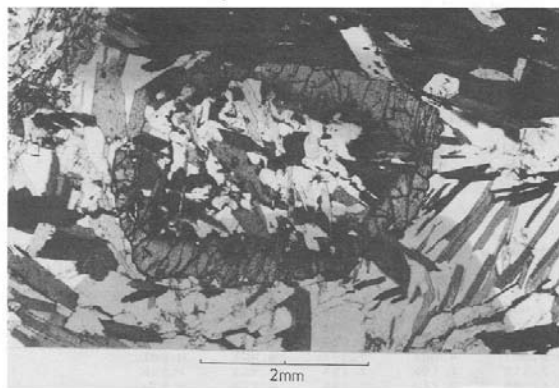
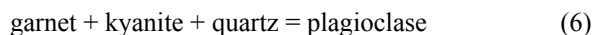


Fig. 10: Randomly oriented biotite and muscovite together with quartz and plagioclase have completely replaced the core of garnet resulting in an atoll structure. Sample K31a, Otjisauna-Süd 156.

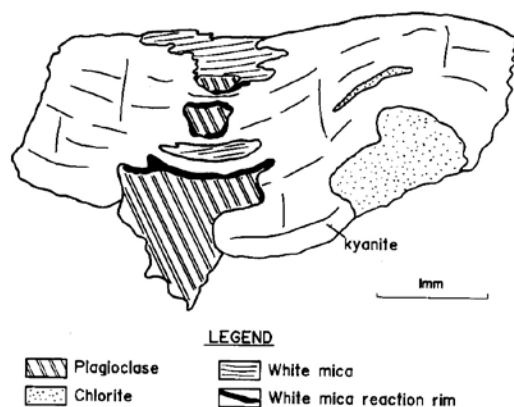


Fig. 11: Deformed kyanite is partly resorbed by undeformed plagioclase, white mica and chlorite. Note the thin reaction rim of white mica between kyanite and plagioclase. Sample K31b, Otjisauna-Süd 156.

has been in progress more or less simultaneously with reaction (4). A thin reaction rim of white mica between the plagioclase and the kyanite (Fig. 11) suggests that some white mica was produced during retrograde metamorphism. Elsewhere retrograde chlorite and white mica have replaced biotite and kyanite.

The breakdown of staurolite at the staurolite-out isograd (Fig. 3) is associated with the formation of elongate sillimanite nodules which are aligned parallel to I_2 . These nodules are pseudomorphs after elongate muscovite porphyroblasts (Fig. 4) rather than staurolite. They are first observed some 1000 to 1500 m before the final disappearance of staurolite indicating that reaction (2) proceeded over a relatively broad band and, therefore, it is slightly divariant. The staurolite-out isograd in Fig. 3 marks the final disappearance of staurolite.

In several samples from zones II and III, deformed kyanite is extensively resorbed by post-tectonic muscovite, while elsewhere muscovite is replaced by sillimanite (Fig. 4). The net reaction thus appears to be that of kyanite reacting to sillimanite via the formation and breakdown of muscovite in two separate subreactions (Carmichael, 1969). Although this is a discontinuous reaction, kyanite is metastable in zones II and III and the kyanite-sillimanite isograd in Fig. 3 only marks the onset of this reaction. The modal decrease of kyanite and the increase of sillimanite from south to north suggest that sillimanite conditions were reached at progressively earlier stages in this direction.

An important consequence of the reaction textures described above is that prograde metamorphism was associated with decompression, because reactions (4), (5) and (6) have low to moderate positive slopes in P-T space (Thompson, 1976b; Ghent, 1976). This is also supported by the progressive replacement of syntectonic kyanite by post-tectonic sillimanite in zones II and III. Therefore, Damaran metapelites of the upper Black Nossob River area have experienced regional metamorphism at relatively high pressures and moderate temperatures during penetrative deformation, followed by

metamorphism at lower pressures and increased temperatures after the deformation.

4. MINERAL CHEMISTRY

4.1 Analytical Techniques

Polished thin sections were prepared from eight samples with representative reaction textures from the four metamorphic zones (Fig. 3). Major element analyses were carried out on garnet, biotite, muscovite, staurolite, and plagioclase using an automated Camebax electron microprobe (15kV acceleration voltage, counting time of 10 seconds) in the Department of Geochemistry at the University of Cape Town. Natural and synthetic mineral standards were used and the data reduced using the Bence-Albee correction procedure. Several analyses were carried out on individual mineral grains and detailed profiles analysed across garnets. Averages of several biotite and plagioclase grains and carefully selected garnet analyses to account for zoning were used

for geothermometry and geobarometry. Representative analyses are listed in Tables 1-4.

4.2 Phase Equilibria

Average mineral analyses of biotite and staurolite as well as average garnet rim compositions are shown in AFM diagrams (Fig. 12). The composition of garnet and biotite in zones I, II, and III is relatively constant and only biotite shows a slight Fe-enrichment with increasing metamorphic grade. The staurolite compositions of zones I and II fall within the garnet-biotite-sillimanite triangle of sample K468 from zone III, suggesting that the absence of staurolite in zone III is indeed the result of staurolite breakdown by the discontinuous reaction (2).

Mineral compositions in the Vaalgras Subgroup of the Ekuja-Otjihangwe Nappe Complex (zone IV) are extremely variable (Fig. 12d). In sample K35c garnet and biotite are so Mg-rich that staurolite compositions of zones I and II fall outside the garnet-biotite-kyanite

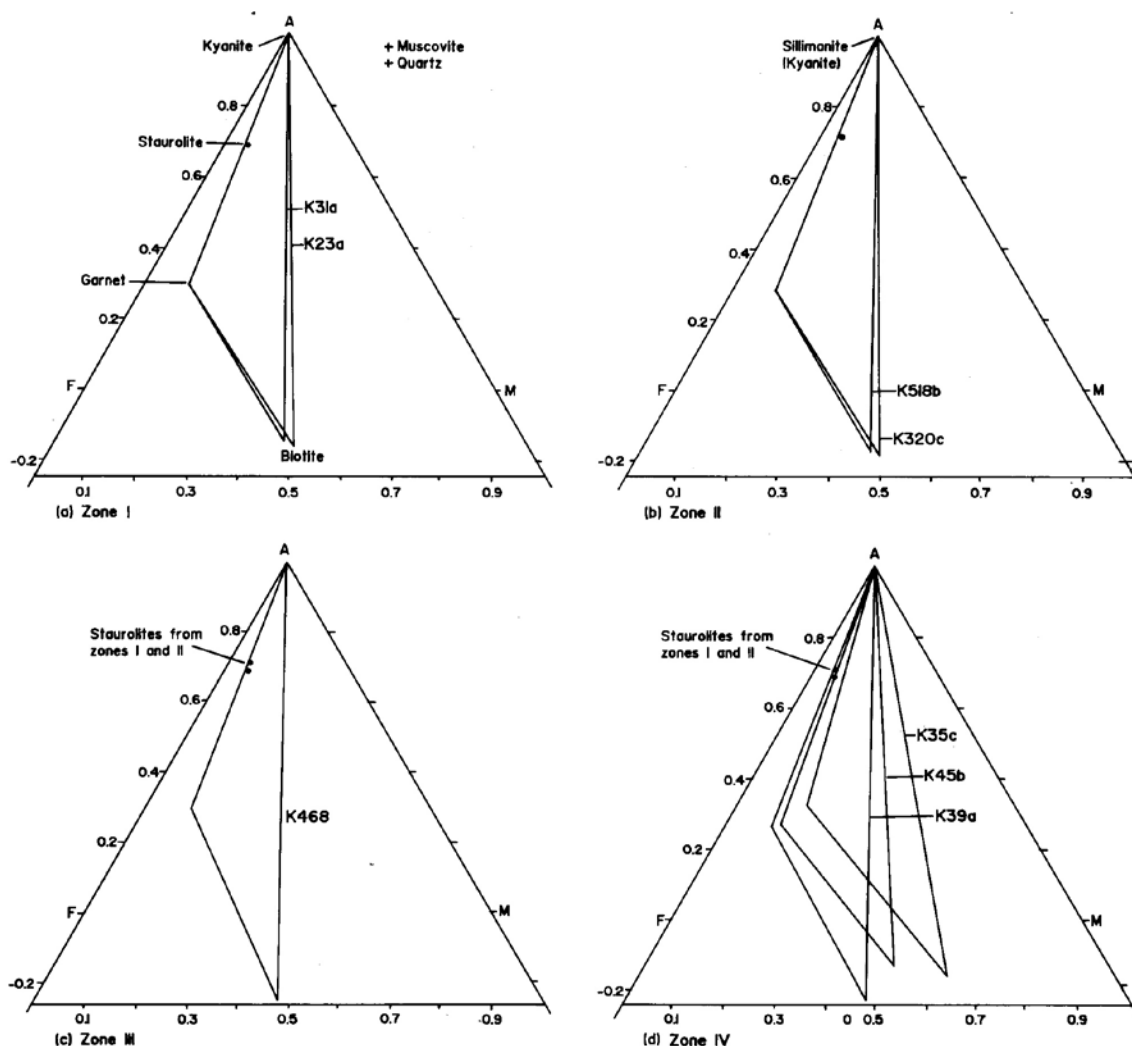


Fig. 12: AFM diagrams after Thompson (1957) illustrating compositions of coexisting minerals. Staurolite compositions from zones I and II are shown in the diagrams for zones III and IV for comparison. Muscovite and quartz are in excess.

TABLE 1: Average garnet analyses.

Sample No	1 K23A	2 K23A	3 K23A	4 K23A	5 K31A	6 K31A	7 K31A	8 K31A	9 K31A	10 K35C
SiO2	37.63	37.14	37.28	37.32	36.78	37.08	36.88	37.05	36.71	37.46
TiO2	0.01	0.26	0.02	0.09	0.09	0.03	0.02	0.02	0.11	0.01
Al2O3	21.20	21.29	21.44	20.90	21.16	21.49	21.17	21.37	21.02	21.35
Cr2O3	-	-	-	-	0.01	0.01	0.01	0.01	0.01	0.01
FeO	33.02	31.68	32.70	30.01	31.92	32.23	32.32	32.11	28.95	24.05
MnO	2.28	4.12	4.23	3.78	3.04	1.31	3.56	2.87	3.10	9.49
MgO	3.52	3.33	3.04	1.90	3.21	3.61	3.08	3.21	1.68	4.50
CaO	3.47	2.74	2.49	6.75	3.51	4.11	2.72	3.38	8.06	3.46
Na2O	-	0.11	-	0.01	0.02	-	0.01	0.01	0.02	-
K2O	-	-	-	-	-	-	-	-	-	-
Total	101.13	100.67	101.20	100.76	99.74	99.87	99.77	100.03	99.66	100.33

* * ATOMIC PROPORTIONS ON THE BASIS OF 12 OXYGENS * *

Si	2.985	2.965	2.970	2.983	2.963	2.965	2.974	2.971	2.961	2.972
Ti	0.001	0.016	0.001	0.005	0.005	0.002	0.001	0.001	0.007	0.001
Al	1.983	2.004	2.014	1.970	2.010	2.026	2.013	2.020	1.999	1.997
Cr	-	-	-	-	0.001	0.001	0.001	0.001	0.001	0.001
Fe	2.191	2.115	2.179	2.006	2.151	2.155	2.180	2.154	1.953	1.596
Mn	0.153	0.279	0.285	0.256	0.207	0.089	0.243	0.195	0.212	0.638
Mg	0.416	0.396	0.361	0.226	0.385	0.430	0.370	0.384	0.202	0.532
Ca	0.295	0.234	0.213	0.578	0.303	0.352	0.235	0.290	0.697	0.294
Na	-	0.017	-	0.002	0.003	-	0.002	0.002	0.003	-
K	-	-	-	-	-	-	-	-	-	-
Sum	8.023	8.026	8.022	8.027	8.028	8.020	8.019	8.018	8.034	8.029
Almandine	0.7171	0.6994	0.7172	0.6542	0.7059	0.7122	0.7198	0.7125	0.6375	0.5215
Spessartine	0.0501	0.0921	0.0940	0.0835	0.0681	0.0293	0.0803	0.0645	0.0691	0.2084
Pyrope	0.1362	0.1310	0.1180	0.0738	0.1265	0.1421	0.1222	0.1269	0.0659	0.1739
Grossular	0.0965	0.0775	0.0700	0.1885	0.0995	0.1164	0.0776	0.0961	0.2274	0.0961
Mg/Mg+Fe	0.1596	0.1578	0.1421	0.1014	0.1520	0.1664	0.1452	0.1512	0.0937	0.2501

DESCRIPTION OF ANALYSES:

- 1 Garnet 1 (rim) in contact with biotite 1-7
- 2 Garnet 2 (rim) resorbed by biotite 8-11
- 3 Garnet 1+2 (rim) in contact with plagioclase 9 and 11-15
- 4 Garnet 1 (core)
- 5 Garnet (core) partly replaced by biotite
- 6 Garnet (rim) in contact with biotite
- 7 Garnet (core and rim) partly replaced by plagioclase
- 8 Garnet (rim) in contact with plagioclase
- 9 Garnet 1 (core)
- 10 Garnet 1 (rim) in contact with biotite

Sample No	11 K35C	12 K35C	13 K39A	14 K39A	15 K45B	16 K45B	17 K45B	18 K320C	19 K320C	20 K320C
SiO2	37.08	37.10	37.05	36.87	37.82	37.24	37.36	37.24	37.04	36.90
TiO2	0.04	0.08	0.03	0.06	0.04	0.02	0.08	-	0.02	-
Al2O3	20.95	21.18	21.10	21.40	21.18	21.18	20.82	21.18	21.36	21.24
Cr2O3	0.01	0.02	0.01	0.01	0.04	0.01	0.01	-	0.04	0.01
FeO	23.52	22.64	35.49	35.67	32.06	31.65	31.57	33.61	33.34	33.50
MnO	10.64	10.79	0.28	0.26	2.17	2.84	3.49	2.59	2.79	4.38
MgO	3.86	3.00	3.56	3.48	3.98	3.79	1.73	3.33	3.20	2.96
CaO	3.77	5.52	2.44	2.35	3.50	3.21	5.21	3.14	3.23	1.90
Na2O	-	-	0.01	0.01	0.01	0.02	0.02	-	0.02	-
K2O	-	-	-	-	-	-	-	-	-	-
Total	99.87	100.33	99.97	100.11	100.80	99.96	100.29	101.09	101.04	100.89

* * ATOMIC PROPORTIONS ON THE BASIS OF 12 OXYGENS * *

Si	2.971	2.963	2.978	2.960	2.995	2.980	3.005	2.968	2.955	2.961
Ti	0.002	0.005	0.002	0.004	0.002	0.001	0.005	-	0.001	-
Al	1.979	1.994	1.999	2.026	1.977	1.998	1.974	1.990	2.009	2.009
Cr	0.001	0.001	0.001	0.001	0.003	0.001	0.001	-	0.003	0.001
Fe	1.576	1.512	2.385	2.395	2.123	2.118	2.123	2.240	2.224	2.248
Mn	0.722	0.730	0.019	0.018	0.146	0.193	0.238	0.175	0.189	0.298
Mg	0.461	0.357	0.426	0.416	0.470	0.452	0.207	0.396	0.380	0.354
Ca	0.324	0.472	0.210	0.202	0.297	0.275	0.449	0.268	0.276	0.163
Na	-	-	0.002	0.002	0.002	0.003	0.003	-	0.003	-
K	-	-	-	-	-	-	-	-	-	-
Sum	8.036	8.035	8.022	8.024	8.014	8.021	8.005	8.037	8.040	8.034
Almandine	0.5112	0.4923	0.7844	0.7901	0.6995	0.6972	0.7037	0.7276	0.7247	0.7339
Spessartine	0.2342	0.2376	0.0063	0.0058	0.0480	0.0634	0.0788	0.0568	0.0614	0.0972
Pyrope	0.1495	0.1163	0.1402	0.1374	0.1547	0.1488	0.0687	0.1285	0.1239	0.1156
Grossular	0.1050	0.1538	0.0691	0.0667	0.0978	0.0906	0.1488	0.0871	0.0900	0.0533
Mg/Mg+Fe	0.2263	0.1910	0.1516	0.1481	0.1811	0.1759	0.0890	0.1501	0.1461	0.1360

DESCRIPTION OF ANALYSES:

- 11 Garnet 1 (rim) in contact with plagioclase
- 12 Garnet 1 (core)
- 13 Garnet (rim) resorbed by biotite
- 14 Garnet (rim) in contact with biotite
- 15 Garnet 1+3 (rim) in contact with biotite
- 16 Garnet 1 (rim) in contact with plagioclase
- 17 Garnet 1 (core)
- 18 Garnet (rim) resorbed by biotite
- 19 Garnet (rim) in contact with biotite
- 20 Garnet 1 (rim) resorbed by plagioclase 1-6

TABLE 1: (continued): Average garnet analyses.

Sample No	21 K320C	22 K320C	23 K468	24 K468	25 K468	26 K518B	27 K518B	28 K518B	29 K518B	30 K518B
SiO2	36.91	36.94	37.00	36.99	37.04	36.76	37.02	37.00	37.39	37.09
TiO2	0.01	0.15	0.01	0.01	0.09	0.08	-	-	-	0.09
Al2O3	21.39	21.28	21.29	21.34	21.19	21.36	21.40	21.54	21.66	21.34
Cr2O3	0.03	0.02	0.01	0.01	0.02	-	-	0.02	-	-
FeO	33.66	29.34	30.69	31.30	29.35	33.49	34.28	33.98	33.75	29.73
MnO	3.81	3.86	6.04	5.67	5.48	3.25	2.62	5.09	3.71	4.38
MgO	3.03	1.53	3.31	2.98	1.73	3.29	3.22	2.57	2.98	1.50
CaO	2.20	7.96	2.55	2.73	6.25	2.70	3.03	1.94	2.91	7.44
Na2O	0.01	0.03	-	-	-	-	-	-	-	0.01
K2O	-	-	-	-	-	-	-	-	-	-
Total	101.05	101.11	100.90	101.03	101.15	100.93	101.57	102.14	102.40	101.58
* * ATOMIC PROPORTIONS ON THE BASIS OF 12 OXYGENS * *										
Si	2.954	2.947	2.958	2.957	2.960	2.941	2.946	2.945	2.952	2.951
Ti	0.001	0.009	0.001	0.001	0.005	0.005	-	-	-	0.005
Al	2.018	2.002	2.006	2.011	1.996	2.015	2.007	2.021	2.016	2.001
Cr	0.002	0.001	0.001	0.001	0.001	-	-	0.001	-	-
Fe	2.253	1.958	2.052	2.093	1.961	2.241	2.281	2.262	2.228	1.978
Mn	0.258	0.261	0.409	0.384	0.371	0.220	0.177	0.343	0.248	0.295
Mg	0.361	0.182	0.394	0.355	0.206	0.392	0.382	0.305	0.351	0.178
Ca	0.189	0.680	0.218	0.234	0.535	0.231	0.258	0.165	0.246	0.634
Na	0.002	0.005	-	-	-	-	-	-	-	0.002
K	-	-	-	-	-	-	-	-	-	-
Sum	8.037	8.045	8.038	8.036	8.036	8.046	8.051	8.043	8.040	8.044
Almandine	0.7359	0.6354	0.6676	0.6826	0.6382	0.7264	0.7364	0.7355	0.7251	0.6411
Spessartine	0.0844	0.0847	0.1331	0.1252	0.1207	0.0714	0.0570	0.1116	0.0807	0.0957
Pyrope	0.1181	0.0590	0.1283	0.1158	0.0670	0.1272	0.1233	0.0991	0.1141	0.0576
Grossular	0.0616	0.2209	0.0711	0.0763	0.1741	0.0750	0.0834	0.0538	0.0801	0.2056
Mg/Mg+Fe	0.1382	0.0850	0.1612	0.1451	0.0951	0.1490	0.1434	0.1188	0.1360	0.0825

DESCRIPTION OF ANALYSES:

- 21 Garnet 3 (rim) in contact with plagioclase 7-10
- 22 Garnet 3 (core)
- 23 Garnet 1+2 (rim) in contact with biotite
- 24 Garnet 1+2 (rim) in contact with plagioclase
- 25 Garnet 1 (core)
- 26 Garnet 2 (close to rim) resorbed by biotite
- 27 Garnet 1 (rim) in contact with biotite
- 28 Garnet 2 (rim) in contact with plagioclase and sillimanite
- 29 Garnet 1 (rim) in contact with plagioclase and kyanite
- 30 Garnet 1 (core)

TABLE 2: Average staurolite analyses.

Sample No	K23A		K320C		K518B	
	RIM	CORE	RIM	CORE	RIM	CORE
SiO2	27.87	28.23	27.69	27.55	27.56	27.69
TiO2	0.66	0.68	0.78	0.78	0.72	0.73
Al2O3	53.74	53.29	54.26	54.17	54.48	54.43
FeO	14.02	14.00	12.79	12.99	13.10	13.40
ZnO	0.88	0.89	1.72	1.63	1.45	1.49
MnO	0.27	0.25	0.27	0.25	0.30	0.33
MgO	1.76	1.95	1.44	1.48	1.50	1.54
Total	99.20	99.29	98.94	98.84	99.11	99.61
* * ATOMIC PROPORTIONS ON THE BASIS OF 23 OXYGENS * *						
Si	3.839	3.884	3.818	3.805	3.795	3.801
Ti	0.068	0.070	0.082	0.080	0.075	0.075
Al	8.724	8.641	8.816	8.818	8.841	8.803
Fe	1.616	1.611	1.474	1.500	1.509	1.538
Zn	0.090	0.090	0.175	0.166	0.148	0.152
Mn	0.032	0.029	0.032	0.030	0.035	0.038
Mg	0.361	0.399	0.295	0.305	0.307	0.315
Sum	14.729	14.724	14.691	14.703	14.709	14.722
Mg/(Mg+Fe)	0.1825	0.1985	0.1669	0.1690	0.1692	0.1700

TABLE 3: Average biotite analyses.

Sample No	1 K23A	2 K23A	3 K31A	4 K31A	5 K35C	6 K35C	7 K39A	8 K39A	9 K45B	10 K320C
SiO2	36.23	35.81	35.39	35.42	37.20	36.52	35.27	35.31	36.53	35.66
TiO2	1.63	1.57	1.62	1.61	1.05	0.90	2.93	2.77	1.73	1.97
Al2O3	18.89	19.93	19.64	19.79	19.28	18.34	19.43	19.97	19.97	20.05
Cr2O3	0.01	-	0.03	0.02	0.02	0.07	0.02	0.02	0.05	0.05
FeO	18.47	18.20	19.14	17.85	13.90	14.06	18.87	19.05	17.63	19.14
MnO	0.04	0.08	0.11	0.08	0.26	0.31	0.02	0.01	0.05	0.06
MgO	11.07	10.50	10.28	10.89	14.38	13.52	9.74	9.51	11.50	10.70
CaO	-	0.04	-	-	-	-	-	-	0.01	-
Na2O	0.34	0.24	0.19	0.22	0.34	0.10	0.18	0.18	0.20	0.29
K2O	8.44	6.42	8.15	8.32	8.31	8.50	8.89	8.11	8.05	8.98
Total	95.12	92.79	94.55	94.20	94.74	92.32	95.35	94.93	95.72	96.90

* * ATOMIC PROPORTIONS ON THE BASIS OF 22 OXYGENS * *

Si	5.459	5.451	5.377	5.373	5.492	5.556	5.333	5.336	5.419	5.308
AlIV	2.541	2.549	2.623	2.627	2.508	2.444	2.667	2.664	2.581	2.692
Ti	0.185	0.180	0.185	0.184	0.117	0.103	0.333	0.315	0.193	0.221
AlVI	0.814	1.027	0.896	0.912	0.848	0.846	0.797	0.893	0.912	0.826
Cr	0.001	-	0.004	0.002	0.002	0.008	0.002	0.002	0.006	0.006
Fe	2.327	2.317	2.432	2.265	1.716	1.789	2.386	2.408	2.187	2.382
Mn	0.005	0.010	0.014	0.010	0.033	0.040	0.003	0.001	0.006	0.008
Mg	2.486	2.382	2.328	2.462	3.164	3.066	2.195	2.142	2.542	2.373
Sum VI	5.818	5.916	5.859	5.835	5.880	5.852	5.717	5.761	5.847	5.816
Ca	-	0.007	-	-	-	-	-	-	0.002	-
Na	0.099	0.071	0.056	0.065	0.097	0.030	0.053	0.053	0.058	0.084
K	1.622	1.247	1.580	1.610	1.565	1.650	1.715	1.564	1.524	1.705
Sum Alk	1.722	1.324	1.636	1.675	1.663	1.679	1.768	1.616	1.583	1.789
Mg/Mg+Fe	0.5165	0.5069	0.4890	0.5209	0.6483	0.6315	0.4791	0.4708	0.5375	0.4990

DESCRIPTION OF ANALYSES:

- 1 Biotite 1-7 in contact with garnet 1
- 2 Biotite 8-11 resorbing garnet 2
- 3 Biotite replacing garnet core
- 4 Biotite in contact with garnet
- 5 Biotite 1-7 in contact with garnet 1
- 6 Biotite 8 (inclusion in plagioclase porphyroblast)
- 7 Biotite resorbing garnet (rim)
- 8 Biotite in contact with garnet
- 9 Biotite 1-6 in contact with garnet 1+3
- 10 Biotite 3-7 resorbing garnet (rim)

Sample No	11 K320C	12 K468	13 K518B	14 K518B
SiO2	35.86	35.21	35.42	35.71
TiO2	2.22	2.24	2.04	2.04
Al2O3	19.84	19.62	19.91	20.29
Cr2O3	0.04	0.02	0.02	0.01
FeO	19.75	19.60	19.86	19.79
MnO	0.06	0.22	0.06	0.10
MgO	10.55	10.18	10.35	10.42
CaO	-	-	-	-
Na2O	0.24	0.17	0.30	0.30
K2O	9.22	9.41	8.83	8.78
Total	97.78	96.67	96.79	97.44

* * ATOMIC PROPORTIONS ON THE BASIS OF 22 OXYGENS * *

Si	5.309	5.290	5.296	5.293
AlIV	2.691	2.710	2.704	2.707
Ti	0.247	0.253	0.229	0.227
AlVI	0.772	0.765	0.805	0.838
Cr	0.005	0.002	0.002	0.001
Fe	2.445	2.463	2.483	2.453
Mn	0.008	0.028	0.008	0.013
Mg	2.328	2.279	2.306	2.302
Sum VI	5.805	5.791	5.834	5.834
Ca	-	-	-	-
Na	0.069	0.050	0.087	0.086
K	1.742	1.804	1.684	1.660
Sum Alk	1.810	1.853	1.771	1.746
Mg/Mg+Fe	0.4877	0.4807	0.4815	0.4841

DESCRIPTION OF ANALYSES:

- 11 Biotite 9+10 in contact with garnet
- 12 Biotite in contact with garnet 1+2
- 13 Biotite resorbing garnet 2 (rim)
- 14 Biotite in contact with garnet 1

TABLE 4: Average plagioclase analyses.

Sample No	1 K23A	2 K31A	3 K31A	4 K31A	5 K35C	6 K35C	7 K45B	8 K320C	9 K320C	10 K468
SiO2	62.44	61.70	63.34	62.94	61.54	62.64	63.49	61.92	62.54	57.81
Al2O3	23.30	23.79	23.23	23.17	24.55	24.04	22.88	23.76	23.52	26.64
FeO	0.19	0.20	0.21	0.05	0.08	0.05	0.13	0.27	0.17	0.36
MgO	-	-	-	-	-	0.01	0.01	-	-	-
CaO	5.20	5.66	5.34	4.40	6.19	4.90	4.56	5.63	5.44	9.07
Na2O	8.67	8.70	7.82	9.20	8.09	8.54	9.14	8.84	8.91	6.40
K2O	0.06	0.07	0.07	0.08	0.05	0.10	0.08	0.05	0.07	0.07
Total	99.86	100.12	100.01	99.84	100.50	100.28	100.29	100.47	100.65	100.35

* * ATOMIC PROPORTIONS ON THE BASIS OF 8 OXYGENS * *

Si	2.771	2.739	2.795	2.788	2.719	2.762	2.801	2.741	2.759	2.584
Al	1.219	1.245	1.209	1.210	1.279	1.250	1.190	1.240	1.223	1.404
Fe	0.007	0.007	0.008	0.002	0.003	0.002	0.005	0.010	0.006	0.013
Mg	-	-	-	-	-	0.001	0.001	-	-	-
Ca	0.247	0.269	0.253	0.209	0.293	0.231	0.216	0.267	0.257	0.434
Na	0.746	0.749	0.669	0.790	0.693	0.730	0.782	0.759	0.762	0.555
K	0.003	0.004	0.004	0.005	0.003	0.006	0.005	0.003	0.004	0.004
Sum	4.994	5.014	4.937	5.004	4.990	4.981	4.998	5.020	5.012	4.994
Anorthite	0.2481	0.2634	0.2728	0.2081	0.2963	0.2393	0.2151	0.2596	0.2513	0.4374
Albite	0.7485	0.7327	0.7229	0.7874	0.7008	0.7548	0.7804	0.7376	0.7448	0.5585
Orthoclase	0.0034	0.0039	0.0043	0.0045	0.0028	0.0058	0.0045	0.0027	0.0039	0.0040

DESCRIPTION OF ANALYSES:

- 1 Plagioclase 9 and 11-15 in contact with garnet 1+2
- 2 Plagioclase replacing garnet (core and rim)
- 3 Plagioclase in contact with garnet
- 4 Plagioclase (core)
- 5 Plagioclase 1+2 in contact with garnet 1
- 6 Plagioclase 6 (core)
- 7 Plagioclase 1-5 in contact with garnet 1
- 8 Plagioclase 1-6 resorbing garnet 1 (rim)
- 9 Plagioclase 7-10 in contact with garnet 3
- 10 Plagioclase 1-3 and 6-10 in contact with garnet 1+3

Sample No	11 K468	12 K518B	13 K518B	14 K518B
SiO2	61.06	61.29	62.51	63.96
Al2O3	24.39	23.98	23.53	22.95
FeO	0.58	0.24	0.15	-
MgO	-	-	-	-
CaO	6.58	6.40	5.85	5.02
Na2O	8.03	8.18	8.52	8.97
K2O	0.08	0.03	0.09	0.10
Total	100.72	100.12	100.65	101.00

* * ATOMIC PROPORTIONS ON THE BASIS OF 8 OXYGENS * *

Si	2.704	2.724	2.758	2.802
Al	1.274	1.257	1.224	1.185
Fe	0.021	0.009	0.006	-
Mg	-	-	-	-
Ca	0.312	0.305	0.277	0.236
Na	0.680	0.705	0.729	0.762
K	0.005	0.002	0.005	0.006
Sum	5.006	5.001	4.997	4.990
Anorthite	0.3103	0.3013	0.2737	0.2349
Albite	0.6852	0.6970	0.7213	0.7595
Orthoclase	0.0045	0.0017	0.0050	0.0056

DESCRIPTION OF ANALYSES:

- 11 Plagioclase 4+9 (inclusion in garnet 1)
- 12 Plagioclase 12+13 in contact with garnet 2 and sillimanite
- 13 Plagioclase in contact with garnet 1 and kyanite
- 14 Plagioclase 10 (core)

triangle. Hence this sample was too Mg-rich for staurolite to have formed in the lower amphibolite facies. The other two samples are more Fe-rich and garnet and biotite compositions in sample K39a from the Hochberg Formation are identical to those of the Kuiseb Formation schists. This suggests that in some schists of zone IV staurolite should have been present before the peak of metamorphism was reached. As this is still within the kyanite stability field, it is concluded that during the peak of metamorphism pressure conditions in the Ekuja-Otjihangwe Nappe Complex were higher than in zones II and III of the Onyati Mountains Schist Belt.

4.3 Garnet Zoning

Representative profiles of zoning in garnet porphyroblasts are illustrated in Figs 13-15. All of them show typical growth zoning (*cf.* Tracey *et al.*, 1976; Trzcien-ski, 1977; Loomis and Nimick, 1982; Dempster, 1985), i.e. they display bell-shaped profiles marked by an increase in almandine, pyrope and Mg/(Mg+Fe) and a simultaneous decrease in grossular and spessartine from core to rim (Fig. 13a). However, some garnets display reverse zoning near the rim (Figs 13b and 14), which is the result of limited diffusion and re-equilibration of the garnet rim with its surroundings during cooling (Tracey *et al.*, 1976; Yardley, 1977b; Dempster, 1985). The effects of reverse zoning in garnet must be accounted for in the application of garnet-biotite geothermometry, else significant underestimates of metamorphic temperatures may be obtained (Hodges and Spear, 1982).

Typical growth zoning without any alteration is illustrated in profile A-B (Fig. 13a) of a garnet shown in Fig. 8. Profile CoD (Fig. 13b) from the same garnet is asymmetrical, displaying reverse zoning near D but not on the opposite side near C. The reason appears to be that biotite has partly resorbed the garnet near C (Fig. 8). This is problematical, because reaction textures suggest that the breakdown of garnet to biotite and kyanite is a prograde reaction (see section 3.2.2.), whereas profile C-D suggests that biotite has resorbed the garnet after retrograde effects have resulted in reverse zoning.

The garnet profile in Fig. 14 shows typical growth zoning in the core and significant reversal of zoning near the rim. An important feature in this example is that reverse zoning of the spessartine component is much wider than that of pyrope and Mg/(Mg+Fe). The former is clearly related to a sharp decrease in grossular component, which is probably related to a significant decrease in pressure during metamorphism (*cf.* Spear and Selverstone, 1983, p. 353). Except for an anomalous pattern in the core, the profile in Fig. 15 displays exactly the same zoning near the rim as that in Fig. 14, suggesting that the sudden drop in grossular content and the reversal of spessartine component are regionally significant.

The relatively small reversals of pyrope and Mg/(Mg+Fe) near the garnet rim in Figs 14 and 15 are

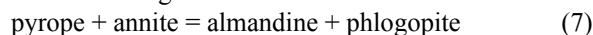
probably the result of retrograde metamorphism. An increase in spessartine component towards the garnet rim is often interpreted as being the result of resorption of garnet by other phases (Yardley, 1977b). However, the garnet profile in Fig. 15 shows that the increase in spessartine component near the rim is wider at B than at A, despite the fact that the garnet has been resorbed by biotite at A and not at B (Fig. 9b). Therefore, the reverse zoning of spessartine in these garnets is not considered to be the result of garnet resorption. The fact that the region in which the increase in spessartine and the decrease in grossular component occurs is much wider than the reversals of pyrope and Mg/(Mg+Fe) suggests that diffusion was still very limited at these metamorphic grades. It is suggested, therefore, that the sudden decrease in grossular component and the increase of spessartine near the garnet rim are the result of equilibrium growth during prograde metamorphism rather than diffusion during cooling. Hoffer (1983) has observed similar reversals in the zoning pattern of spessartine and almandine at the staurolite-in isograd to the south-west of Windhoek, which he has also interpreted as being due to equilibrium growth.

The garnet of Fig. 9b has biotite, quartz and plagioclase partly replacing its core and Fig. 15 clearly demonstrates that this has resulted in another type of diffusion zoning. Significant Ca has been removed from the garnet and is obviously taken up by plagioclase. At the same time almandine, pyrope, and Mg/(Mg+Fe) show a marked increase in the resorbed core. The high grossular component and low Mg/(Mg+Fe) of the original garnet core suggests that growth of this core took place at significantly lower temperature and higher pressure conditions than its breakdown (*cf.* Spear and Selverstone, 1983). In general, therefore, garnet zoning patterns support the textural evidence for prograde decompression in the upper Black Nossob River area.

5. GEOTHERMOMETRY AND GEOBAROMETRY

5.1 Garnet-biotite Geothermometry

The garnet-biotite geothermometer is based on the cation exchange reaction



Although several calibrations of this geothermometer have been proposed, the only experimental calibration is that of Ferry and Spear (1978), which gives reasonable temperature estimates for the lower and the middle amphibolite facies (Ghent *et al.*, 1979; Hodges and Spear, 1982; Kasch, 1983a,b,c). It does not, however, account for the effect of significant amounts of grossular and spessartine in garnet and Al^{VI} and Ti in biotite.

Hodges and Spear (1982) have proposed an empirical correction for the non-ideal behaviour of garnet solid solutions based on samples from an area near the Al₂SiO₅ invariant point. However, their definition of the

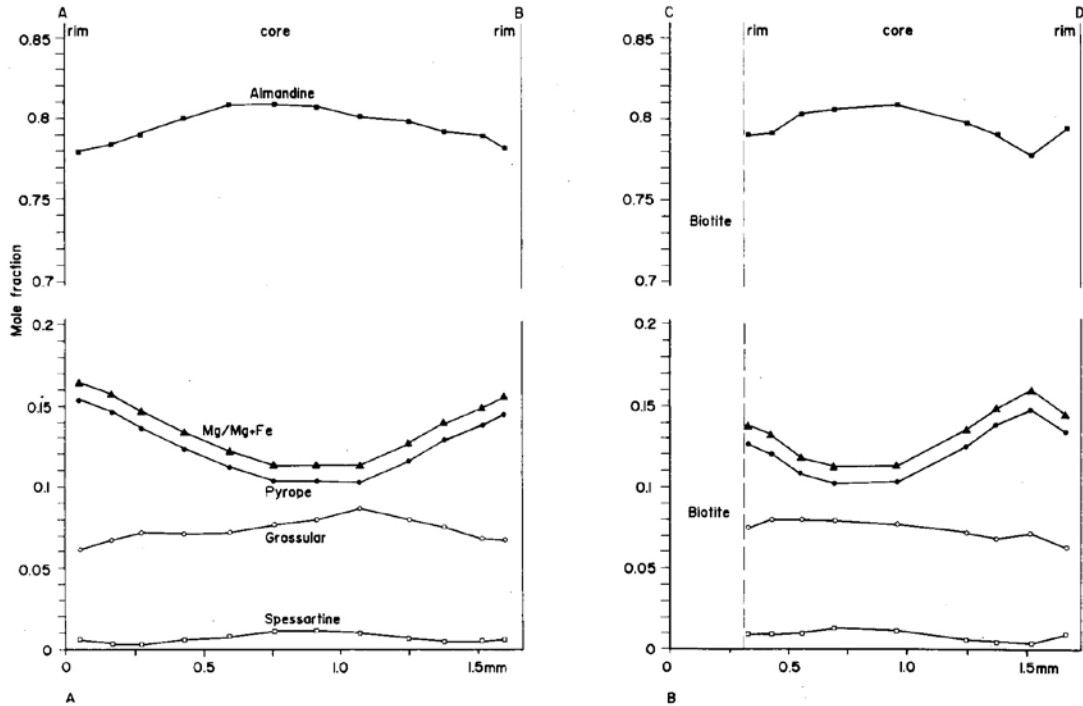


Fig. 13: Garnet endmember and Mg/(Mg+Fe) profiles for partly resorbed garnet shown in Fig. 8. Sample K39a, Hochberg Formation.

- (a) Profile A-B illustrates typical growth zoning.
 (b) Profile C-D illustrates growth zoning in core and reverse zoning near rim at D.

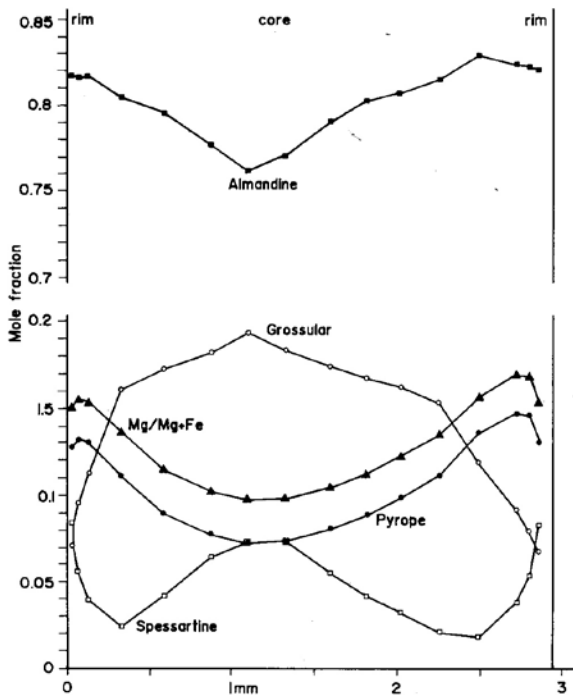


Fig. 14: Garnet endmember and Mg/(Mg+Fe) profile for a garnet in sample K23a, Kuiseb Formation, Otjisauna-Nord 157. Profile illustrates typical growth zoning in the core and reverse zoning near the rim of garnet.

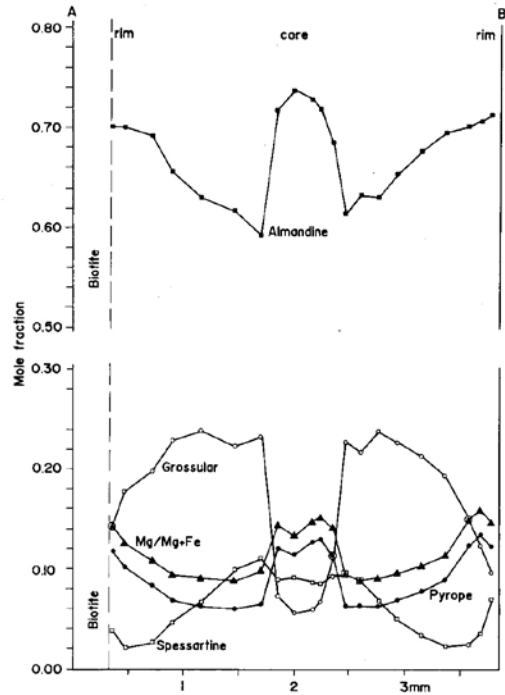


Fig. 15: Garnet endmember and Mg/(Mg+Fe) profile for an internally resorbed garnet shown in Fig. 9b. Sample K31a, Kuiseb Formation Otjisauna-Süd 156. The basic growth zoning is still preserved, although it has been strongly modified by resorption and retrograde effects.

distribution coefficient, K_D , differs from the original one by Ferry and Spear (1978) and if applied to the upper Black Nossob River area, it yields underestimates of metamorphic temperatures of the order of several hundred degrees. An attempt has been made to apply this correction to sample K39a from the Hochberg Formation, but using a K_D similar to that originally defined by Ferry and Spear (1978). This method yields a slightly higher estimate than the original Ferry and Spear geothermometer, the difference being 27°C for sample K39a (compare curves labelled 'a' and 'c' for K39a in Fig. 16). A similar correction has not yet been attempted for the other samples. The experimental uncertainty of the garnet-biotite geothermometer is $\pm 50^\circ\text{C}$ (Ferry and Spear, 1978).

5.2 Garnet-plagioclase- Al_2SiO_5 -quartz Geobarometry

Ghent (1976) has applied the reaction
grossular + 2 Al_2SiO_5 + quartz = 3 anorthite (8)
as a geobarometer using available thermochemical data. Schmidt and Wood (1976) have used additional constraints to calibrate this reaction for sillimanite-bearing samples and Waters (in Kasch, 1983b,c) has followed a similar procedure for the kyanite reaction. Using more recent experimental data, Newton and Haselton (1981) have proposed a new calibration for reaction (8), and Hodges and Spear (1982) have presented an empirical correction for non-ideal solid solution in garnet and plagioclase. In order to be consistent with previous applications of the garnet-plagioclase geobarometer in the Damara Orogen, the calibrations of Schmidt and Wood (1976) and Waters (in Kasch, 1983b,c) are used here. However, the correction of Hodges and Spear (1982) for the non-ideal behaviour of natural phases has been applied, and this appears to give reasonable pressure estimates. Furthermore, pressures were also calculated for the sillimanite-bearing samples using the calibration of Newton and Haselton (1981) and the correction procedure of Hodges and Spear (1982). This method yielded pressure estimates which are approximately 0.5kb lower than the method of Waters (in Kasch, 1983b,c) for sample K518b and K468.

The kyanite equilibrium for reaction (8) was used to calculate pressures for those samples containing kyanite only (K23a, K31a of zone I and K35c, K39a, K45b of zone IV). For samples containing both kyanite and sillimanite (K320c from zone II and K518b from the staurolite-out isograd) the kyanite equilibrium was used to calculate the pressure for garnet-plagioclase in contact with or close to kyanite, and the sillimanite equilibrium was used to calculate the pressure for garnet-plagioclase in contact with sillimanite. For sample K468 (zone III) in which much sillimanite and only one relic of kyanite is present, the pressure was calculated using the sillimanite equilibrium only.

The experimental uncertainties for the garnet-pla-

gioclase geobarometer are $\pm 1.2\text{kb}$ (Waters, 1979, in Kasch, 1983b,c). However, if uncertainties in analytical errors and activity-composition relationships are added, the overall error is probably of the order of 1.5kb (Hodges and Spear, 1982).

5.3 Regional P-T Variations

Due to reverse zoning near garnet rims it is expected that calculations which employ rim compositions will not give peak metamorphic temperatures (Tracey *et al.*, 1976). Average garnet compositions were, therefore, first computed using analyses at various distances away from the rim. These were then used together with averaged compositions of biotite in contact with garnet to calculate temperatures. It was found that analyses between 30 and 40 μ away from the rim give the highest and most reasonable temperature estimates for most samples. The results are illustrated in P-T diagrams in Fig. 16. In general garnet rims which show resorption by biotite (curves labeled 'a'), give slightly higher temperatures than those which show no reaction (curves labeled 'b'). This accords with the fact that resorbed garnets are the result of the prograde decompression reaction (4) and, therefore, reflect peak metamorphic conditions.

Calculated garnet-plagioclase pressures are illustrated in Fig. 16. No clearly defined retrograde effects have been observed in the grossular profiles of the garnets (Figs 13-15) and, therefore, pressures were calculated from average rim compositions in contact with plagioclase. However, reaction textures as well as garnet zoning suggest that there was a late to post-tectonic decrease in metamorphic pressure and there is no reason to believe why pressure should have increased after the peak of metamorphism. In fact an increase in pressure during retrograde metamorphism would show up as an increase in grossular component near the garnet rim, which is not observed in the garnet profiles. Conversely a decrease in pressure would result in a decrease in grossular component near garnet rims, which cannot be distinguished from the general decrease in grossular component from core to rim (Figs 13-15). Consequently the pressures obtained in Fig. 16 should be regarded as minimum pressures, because the garnet rims may have re-equilibrated slightly during cooling. Unfortunately the extent of a possible re-equilibration is unknown and it may even vary from one sample to another.

In a few samples from the Kuiseb Formation it was possible to distinguish between plagioclase in contact with resorbed garnet (curves labelled '1') and plagioclase in contact with unresorbed garnet (curves labelled '2'). For K31a and K320c the unresorbed portions of garnets yielded pressure estimates only slightly higher than those for the resorbed portions (see Fig. 16). In sample K518b, however, plagioclase in contact with garnet and kyanite yields a pressure estimate which is 1.5kb higher than plagioclase in contact with garnet

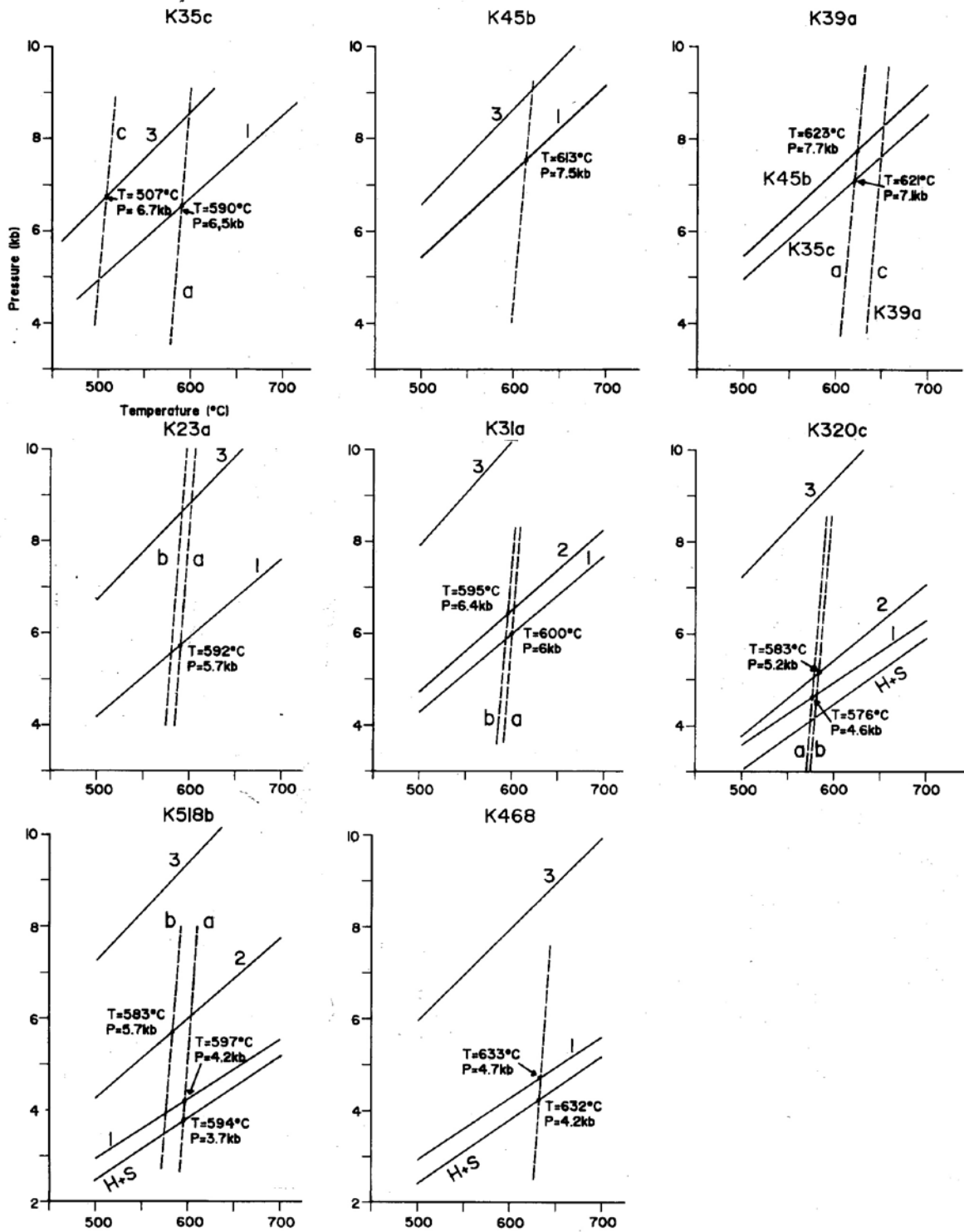


Fig. 16: P-T diagrams illustrating estimates of garnet-biotite temperature (dashed curves) and garnet-plagioclase pressure (solid curves). Samples K35c, K45b, and K39a are from Hochbeg hill of the Ekuja-Otjihangwe Nappe Complex (zone IV). All other samples are from the Onyati Mountains Schist Belt: K23a and K31a (zone I); K320c (zone II); K468 (zone III); K518b (staurolite-out isograd). Uncertainties of $\pm 50^{\circ}\text{C}$ and $\pm 1.5\text{kb}$ for temperature and pressure respectively have been omitted for clarity. H+S: garnet-plagioclase equilibrium corrected for non-ideal solid solution (after Hodges and Spear, 1982).

and sillimanite. Garnets in contact with plagioclase and sillimanite are resorbed extensively by biotite and sillimanite. For sample K320c as well as K518b the kyanite equilibrium relationship for reaction (8) was used to calculate curve 2, while the sillimanite equilibrium relationship was used to calculate curve 1.

Two samples from the Vaalgras Subgroup which contain plagioclase (K35c and K45b) were used to obtain pressure estimates for the Ekuja-Otjihangwe Nappe Complex (Fig. 16). In addition, the garnet-plagioclase curves for these samples intersect the garnet-biotite curve of K39a at 7.1 and 7.7kb respectively and at approximately 622°C.

P-T estimates which reflect peak metamorphic conditions in various parts of the upper Black Nossob River area are summarized in Fig. 17. From this P-T diagram the following points are evident:

- There is a distinct decrease in pressure across the kyanite-sillimanite isograd from zone I in the south to zones II and III in the northern part of the Onyati Mountains Schist Belt.
- Temperatures obtained for zones I and II are more or less identical, but significantly higher temperatures were recorded for zone III. This is supported by the staurolite-out isograd separating zone II from zone III.
- During the peak of metamorphism the highest pressures prevailed in the Ekuja-Otjihangwe Nappe Complex. Therefore, there is also a distinct decrease in pressure from east to west in the upper Black Nossob River area.
- The highest garnet-biotite temperatures were obtained for samples from the Ekuja-Otjihangwe Nappe Complex and zone III of the Onyati Mountains Schist Belt, which is in accordance with the absence of staurolite in these two areas.
- The pressure estimates are in excellent agreement

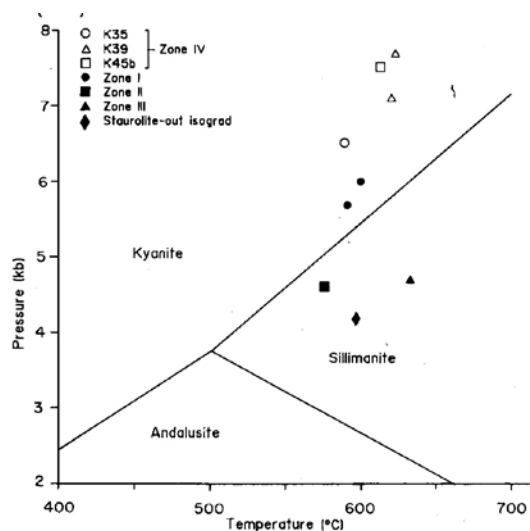


Fig. 17: P-T diagram summarizing the peak metamorphic temperatures and pressures for all the samples.

with the kyanite and sillimanite stability fields of Holdaway (1971).

5.4 Tectonothermal Evolution

In addition to garnet rim compositions, average core compositions were used together with plagioclase inclusions and matrix plagioclase to obtain early metamorphic pressure estimates. For most plagioclase inclusions pressure estimates are very similar to those of matrix plagioclase in contact with garnet rim. However, the plagioclase inclusions show strong compositional variations and many of them are extremely rich in anorthite component (Figure 18). These compositions are unusual for pelitic schists metamorphosed under greenschist to amphibolite facies conditions. It is suggested, therefore, that during the peak of metamorphism most plagioclase inclusions have re-equilibrated with the relatively high grossular component of the garnet core regions.

One exception to this strong compositional variation of plagioclase inclusions is sample K468 from zone III, in which they are only slightly enriched in anorthite component as compared with matrix plagioclase. However, in this sample matrix plagioclase is more calcic than in all the other samples (Figure 18). Two inclusions in K468 are much more sodic than matrix plagioclase, and it is suggested that these are least re-equilibrated. Using these two plagioclase inclusions together with the average core composition of garnet a much higher pressure estimate is obtained (curve 3 for K468 in Fig. 16).

For most other samples the early metamorphic pressure was calculated using average garnet core compositions in conjunction with the average composition of matrix plagioclase (curves labelled '3' in Fig. 16). In sample K518b the larger matrix plagioclase grains are zoned with anorthite content increasing from core to rim. Obviously only the core of these plagioclases could have been in equilibrium with the garnet core during the early stages of metamorphism and, therefore, plagioclase core compositions were used to calculate the early metamorphic pressure for this sample. For sample K35c (zone IV) the early metamorphic pressure was calculated from the average core compositions of a

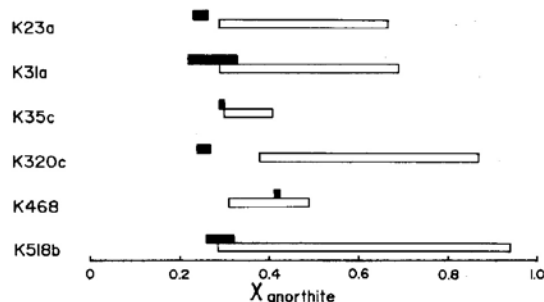


Fig. 18: Compositional variation in matrix plagioclase (solid bars) and plagioclase inclusions in garnet (open bars).

large syntectonic garnet and a large syntectonic plagioclase. The plagioclase porphyroblast is approximately 23mm long and 5 mm wide and almost unzoned. Nevertheless, the average core composition was used for the calculation of the garnet-plagioclase curve.

Without exception the garnet-plagioclase equilibrium curves for garnet core compositions are at higher pressures than those for garnet rim compositions. In the absence of original biotite inclusions in garnet it is impossible to estimate the temperatures at which the garnets started to grow. However, a biotite inclusion was found in the central parts of the large plagioclase porphyroblast in sample K35c, and it is assumed that biotite of similar composition was in equilibrium with the garnet core. Using this biotite in conjunction with the average garnet core composition, a garnet-biotite equilibrium curve was calculated which intersects the garnet-plagioclase curve for the core of the same syntectonic garnet and the large plagioclase porphyroblast at 507°C and 6.7kb (curves labelled 'c' and '3' in Fig. 16). If this P-T estimate is correct, then it is obvious that at least the western portions of the Ekuja-Otjihangwe Nappe Complex experienced more or less isobaric heating during prograde metamorphism.

Oxygen isotope temperatures for the garnet isograd in the Southern Margin Thrust Belt range between 483°C and 540°C (Hoernes and Hoffer, 1979), which is in good agreement with the temperature estimate for the garnet core of sample K35c. Therefore, it is assumed that during initiation of garnet growth in the schists of the Onyati Mountains Schist Belt the temperature was also of the order of 500°C. The curves labelled '3' in Fig. 16 thus indicate that during the initial stages of garnet growth in the Onyati Mountains Schist Belt the pressure was distinctly higher than during the peak of metamorphism. This decompression during prograde metamorphism is best recorded in sample K518b, for which the following P-T estimates were obtained (the uncertainties being ± 1.5 kb and $\pm 50^\circ\text{C}$ respectively):

- (a) 7.2kb at 500°C during the initial stages of garnet growth.
- (b) 5.7kb at 583°C during the final stages of garnet growth (in the kyanite stability field).
- (c) 4.2kb at 597°C during the peak of metamorphism (garnet breakdown in the sillimanite stability field).

It should be pointed out that kyanite may not have been present during the early stages of garnet growth and, therefore, the equilibrium relationship for reaction (8) would no longer be applicable. This would mean that the results can only be regarded as maximum pressures. However, the quantitative P-T estimates for all the samples from the Onyati Mountains Schist Belt suggest that prograde metamorphism of the Kuiseb schists was associated with a regional decompression. This is in good agreement with the observed reaction textures as well as garnet zoning profiles.

6. DISCUSSION AND CONCLUSIONS

Results from this study have provided new insights into the regional metamorphism and the tectonothermal evolution of the southern Damara Orogen.

Three metamorphic zones are distinguished in the Onyati Mountains Schist Belt, which are separated by the kyanite-sillimanite and the staurolite-out isograd respectively (Fig. 3). Phase equilibria suggest that there is an increase in metamorphic grade and a decrease in pressure from zone I in the south to zone III in the north. Furthermore, the absence of staurolite in garnet-biotite-kyanite schists in zone IV indicates that the temperature in this area was similar to that of zone III, but the pressure was distinctly higher.

These observations are supported by garnet-biotite geothermometry and garnet-plagioclase geobarometry. Temperature estimates are the same for zones I and II and only show an increase across the staurolite-out isograd from zone II into zone III (Fig. 17). On the other hand pressure estimates for zones II and III are similar while distinctly higher pressures were recorded for zone I. Therefore, the kyanite-sillimanite isograd is due to a decrease in pressure and not an increase in temperature, while the staurolite-out isograd between zones II and III indicates an increase in temperature at constant pressure (Fig. 17). Furthermore, during the peak of metamorphism the highest pressures prevailed in the Ekuja-Otjihangwe Nappe Complex, which has also experienced slightly higher temperatures than zone I and zone II of the Onyati Mountains Schist Belt.

The general increase in temperature and decrease in pressure from south to north in the Onyati Mountains Schist Belt is consistent with the change in P-T conditions across the Khomas Zone (*cf.* Hoffer, 1978; Sawyer, 1981; Kasch, 1983a). The fact that the highest peak metamorphic pressure estimates were obtained for the Ekuja-Otjihangwe Nappe Complex suggests that this represents the lowest structural unit in the upper Black Nossob River area. This is in agreement with structural and lithostratigraphic observations made by Kasch (1986).

Metamorphic reaction textures and garnet zoning profiles suggest that the Onyati Mountains Schist Belt has experienced decompression during the final stages of prograde metamorphism. The nature of the kyanite-sillimanite isograd and the persistence of metastable kyanite in zones II and III of the Onyati Mountains Schist Belt support these findings. An attempt was made to obtain early syntectonic P-T estimates, but various assumptions had to be made. Nevertheless, the quantitative P-T estimates for all the samples from the Onyati Mountains Schist Belt suggest that prograde metamorphism of the Kuiseb schists was associated with extensive regional decompression. In contrast, results from the Vaalgras Subgroup suggest that the Ekuja-Otjihangwe Nappe Complex experienced more or less isobaric heating during garnet growth. However, reaction tex-

tures suggest that during the peak of metamorphism the Ekuja-Otjihangwe Nappe Complex also experienced some decompression.

If the assumptions made are correct, then the early metamorphic history of the Ekuja-Otjihangwe Nappe Complex differs from that of the Onyati Mountains Schist Belt. These results are in agreement with structural observations that the Hochberg Thrust is a major tectonic boundary which separates the Ekuja-Otjihangwe Nappe Complex from overlying units of the Khomas Zone.

In the Omitara area to the south-east of the upper Black Nossob River area, garnet, staurolite, kyanite, biotite and muscovite grew during an early syntectonic event as well as after the deformation. In addition, microtextural evidence suggests that the metamorphic grade decreased considerably between the two phases of mineral growth, which is confirmed by a quantitative reconstruction of the metamorphic history (Kasch, 1983b,c). However, in the upper Black Nossob River area no evidence has been found for a decrease in temperature between the two phases of mineral growth. It has to be accepted, therefore, that this area has been affected by a single, prolonged event of prograde metamorphism, as suggested by Hoffer (1978) for the Damara Orogen as a whole.

7. ACKNOWLEDGEMENTS

I would like to thank Mr. K.H. Hoffmann for reviewing the original manuscript and my wife Annemarie for drafting of the diagrams. Funding of this project by the Committee for Research Priorities of SWA/Namibia is gratefully acknowledged. The tables of mineral analyses were printed on the Epson GQ3500 laser printer which was kindly made available by The Matrix in Windhoek.

REFERENCES

- Carmichael, D.M. 1969. On the mechanism of prograde metamorphic reactions in quartz-bearing pelitic rocks. *Contr. Miner. Petrol.*, **20**, 244-267.
- Dempster, T.J. 1985. Garnet zoning and metamorphism of the Barrovian type area, Scotland. *Contr. Miner. Petrol.*, **89**, 30-38.
- Ferry, J.M., and Spear, F.S. 1978. Experimental calibration of the partitioning of Fe and Mg between biotite and garnet. *Contr. Miner. Petrol.*, **66**, 113-117.
- Ghent, E.D. 1976. Plagioclase-garnet- Al_2SiO_5 -quartz: a potential geobarometer-geothermometer. *Am. Miner.*, **61**, 710-714.
- Ghent, E.D., Robbins, D.B. and Stout, M.Z. 1979. Geothermometry, geobarometry, and fluid compositions of metamorphosed calc-silicates and pelites, Mica Creek, British Columbia. *Am. Miner.*, **64**, 874-885.
- Hodges, K.V. and Spear, F.S. 1982. Geothermometry, geobarometry and the Al_2SiO_5 triple point at Mt. Moosilauke, New Hampshire. *Am. Miner.*, **67**, 1118-1134.
- Hoernes, S. and Hoffer, E. 1979. Equilibrium relations of prograde mineral assemblages: A stable isotope study of rocks of the Damara Orogen, from Namibia. *Contr. Miner. Petrol.*, **68**, 377-389.
- Hoffer, E. 1978. On the "late" formation of paragonite and its breakdown in pelitic rocks of the southern Damara Orogen (Namibia). *Contr. Miner. Petrol.*, **67**, 209-219.
- Hoffer, E. 1983. Compositional variations of minerals in metapelites involved in low- to medium grade isograd reactions in the southern Damara Orogen, Namibia, South West Africa, 745-765. In: Martin, H., and Eder, F.W., Eds, *Intracontinental Fold Belts - Case Studies in the Variscan Belt of Europe and the Damara Belt in Namibia*. Springer-Verlag, Berlin, 945 pp.
- Holdaway, M.J. 1971. Stability of andalusite and the aluminium silicate phase diagram. *Am. J. Sci.*, **271**, 97-131.
- Kasch, K.W. 1983a. Regional P-T variations in the Damara Orogen with particular reference to early high-pressure meta.morphism along the southern margin. *Spec. Publ. geol. Soc. S. Afr.*, **11**, 243-253.
- Kasch, K.W. 1983b. Tectonothermal evolution of the southern Damara Orogen. *Spec. Publ. geol. Soc. S. Afr.*, **11**, 255-265.
- Kasch, K.W. 1983c. The structural geology, metamorphic petrology and tectonothermal evolution of the southern Damara Belt around Omitara, SWA/Namibia. *Bull. Precambrian Res. Unit, Univ. Cape Town*, **27**, 333 pp.
- Kasch, K.W. 1986. Tectonic subdivision, lithostratigraphy and structural geology of the upper Black Nossob River area. *Communs geol. Surv. SW Africa/Namibia*, **2**, 117-129.
- Loomis, T.P., and Nimick, F.B. 1982. Equilibrium in Mn-Fe-Mg aluminous pelitic compositions and the equilibrium growth of garnet. *Can. Miner.*, **20**, 393-410.
- Newton, R.C., and Haselton, H.T. 1981. Thermodynamics of the garnet-plagioclase- Al_2SiO_5 -quartz geobarometer, 131-147. In: Newton, R.C. et al., Eds, *Thermodynamics of Minerals and Melts*. Springer-Verlag, New York.
- Sawyer, E. W. 1981. Damaran structural and metamorphic geology of an area south-east of Walvis Bay, South West Africa/Namibia. *Memoir geol. Surv. S.W Africa/Namibia*, **7**, 94 pp.
- Schmidt, R. and Wood, B.J. 1976. Phase relationships in granulitic metapelites from the Ivrea-Verbano Zone (Northern Italy). *Contr. Miner. Petrol.*, **54**, 255-279.
- Spear, F.S., and Selverstone, J. 1983. Quantitative poT paths from zoned minerals: theory and tectonic applications. *Contr. Miner. Petrol.*, **83**, 348-357.
- Thompson, A.B. 1976a. Mineral reactions in pelitic

- rocks: I. Prediction of P-T-X(Fe-Mg) phase relations. *Am. J. Sci.*, **276**, 401-424.
- Thompson, A.B. 1976b. Mineral reactions in pelitic rocks: II. Calculation of some P-T-X(Fe-Mg) phase relations. *Am. J. Sci.*, **276**, 425-454.
- Thompson, J.B., Jr. 1957. The graphical analysis of mineral assemblages in pelitic schists. *Am. Miner.*, **42**, 842-858.
- Tracy, R.J., Robinson, P., and Thompson, A.B. 1976. Garnet composition and zoning in the determination of temperature and pressure of metamorphism, central Massachusetts. *Am. Miner.*, **61**, 762-775.
- Vernon, R.H. 1978. Porphyroblast-matrix microstructural relationships in deformed metamorphic rocks. *Geol. Rdsch.*, **67**, 288-305.
- Trzcienski, W.E., Jr. 1977. Garnet zoning - product of a continuous reaction. *Can. Miner.*, **15**, 250-256.
- Yardley, S.W.D. 1977a. The nature and significance of the mechanism of sillimanite growth in the Connemara schists, Ireland. *Contr. Miner. Petrol.*, **65**, 53-58.
- Yardley, S.W.D. 1977b. An empirical study of diffusion in garnet. *Am. Miner.*, **62**, 793-800.
- Zwart, H.J. 1962. On the determination of polymetamorphic mineral associations and its application to the Bosost area (Central Pyrenees). *Geol. Rdsch.*, **52**, 38-65.